Parabolic pulse generation with active or passive dispersion decreasing optical fibers

Christophe Finot[1*], Benoit Barviau[1], Guy Millot[1], Alexej Guryanov, [2] Alexej Sysoliatin [3], and Stefan Wabnitz [1]

[1] *Institut Carnot de Bourgogne, UMR 5029 CNRS-Université de Bourgogne, 9 Av. A. Savary, Dijon, France*
[2] *Institute of Chemistry of High Purity Substances, 49 Tropinin Street, Nizhny Novgorod, 603950, Russia*
[1] *Fiber Optics Research Center at GPI, 38 Vavilov Street, Moscow, 119333, Russia*
* Corresponding author: *christophe.finot@u-bourgogne.fr*

Abstract: We experimentally demonstrate the possibility to generate parabolic pulses via a single dispersion decreasing optical fiber with normal dispersion. We numerically and experimentally investigate the influence of the dispersion profile, and we show that a hybrid configuration combining dispersion decrease and gain has several benefits on the parabolic generated pulses.

OCIS codes: (060.4370) Nonlinear optics, fibers; (320.5540) Pulse shaping; (060.5530) Pulse propagation and solitons.

References and links

1. J. M. Dudley, C. Finot, G. Millot, and D. J. Richardson, "Self-similarity and scaling phenomena in nonlinear ultrafast optics," Nat. Phys. **3,** 597-603 (2007).
2. M. E. Fermann, V. I. Kruglov, B. C. Thomsen, J. M. Dudley, and J. D. Harvey, "Self-similar propagation and amplification of parabolic pulses in optical fibers," Phys. Rev. Lett. **84**, 6010-6013 (2000).
3. C. Finot, S. Pitois, G. Millot, C. Billet, and J. M. Dudley, "Numerical and experimental study of parabolic pulses generated via Raman amplification in standard optical fibers," IEEE J. Sel. Top. Quantum Electron. **10**, 1211-1218 (2004).
4. C. Finot, and G. Millot, "Synthesis of optical pulses by use of similaritons," Opt. Express **12**, 5104-5109 (2004).
5. C. Finot, S. Pitois, and G. Millot, "Regenerative 40-Gb/s wavelength converter based on similariton generation," Opt. Lett. **30**, 1776-1778 (2005).
6. F. Parmigiani, C. Finot, K. Mukasa, M. Ibsen, M. A. F. Roelens, P. Petropoulos, and D. J. Richardson, "Ultra-flat SPM-broadened spectra in a highly nonlinear fiber using parabolic pulses formed in a fiber Bragg grating," Opt. Express **14**, 7617-7622 (2006).
7. C. Finot, L. Provost, P. Petropoulos, and D. J. Richardson, "Parabolic pulse generation through passive nonlinear pulse reshaping in a normally dispersive two segment fiber device," Opt. Express **15**, 852-864 (2007).
8. T. Hirooka, and M. Nakazawa, "Parabolic pulse generation by use of a dispersion-decreasing fiber with normal group-velocity dispersion," Opt. Lett. **29**, 498-500 (2004).
9. A. Plocky, A. A. Sysoliatin, A. I. Latkin, V. F. Khopin, P. Harper, J. Harrison, and S. K. Turitsyn, "Experiments on the generation of parabolic pulses in waveguides with length-varying normal chromatic dispersion," JETP Lett. **85**, 319-322 (2007).
10. B. Kibler, C. Billet, P. A. Lacourt, R. Ferrière, L. Larger, and J. M. Dudley, "Parabolic pulse generation in comb-like profiled dispersion decreasing fibre," Electron. Lett. **42**, 965-966 (2006).
11. A. Latkin, S. K. Turitsyn, and A. Sysoliatin, "On the theory of parabolic pulse generation in tapered fibre," Opt. Lett. **32**, 331-333 (2007).
12. M. Nakazawa, E. Yoshida, H. Kubota, and Y. Kimura, "Generation of a 170 fs, 10 GHz transform-limited pulse train at 1.55 um using a dispersion-decreasing, erbium-doped active soliton compressor," Electron. Lett. **30**, 2038-2039 (1994).
13. T. Kogure, J. H. Lee, and D. J. Richardson, "Wavelength and duration-tunable 10-GHz 1.3-ps pulse source using dispersion decreasing fiber-based distributed Raman amplification," IEEE Photon. Technol. Lett. **16**, 1167-1169 (2004).
14. D. Méchin, S. H. Im, V. I. Kruglov, and J. D. Harvey, "Experimental demonstration of similariton pulse compression in a comblike dispersion-decreasing fiber amplifier," Opt. Lett. **31**, 2106-2108 (2006).
15. G. P. Agrawal, *Nonlinear Fiber Optics, Third Edition* (San Francisco, CA, Academic Press, 2001).
16. V. A. Bogatyrev, M. M. Bubnov, E. M. Dianov, A. S. Kurkov, P. V. Mamyshev, A. M. Prokhorov, S. D. Rumyantsev, V. A. Semenov, S. L. Semenov, A. A. Sysoliatin, S. V. Chernikov, A. N. Gur'yanov, G. G.

#87110 - $15.00 USD Received 4 Sep 2007; revised 1 Oct 2007; accepted 3 Oct 2007; published 15 Nov 2007

Devyatykh, and S. I. Miroshnichenko, "A single-mode fiber with chromatic dispersion varying along the length," J. Lightwave Technol. **9**, 561-565 (1991).
17. C. Finot, G. Millot, C. Billet, and J. M. Dudley, "Experimental generation of parabolic pulses via Raman amplification in optical fiber," Opt. Express **11**, 1547-1552 (2003).
18. C. Finot, "Influence of the pumping configuration on the generation of optical similaritons in optical fibers," Opt. Commun. **249**, 553-561 (2005).
19. R. Trebino, *Frequency-Resolved Optical Gating : the measurement of ultrashort laser pulses* (Norwell, MA, Kluwer Academic Publishers, 2000).
20. V. I. Kruglov, A. C. Peacock, J. M. Dudley, and J. D. Harvey, "Self-similar propagation of high-power parabolic pulses in optical fiber amplifiers," Opt. Lett. **25**, 1753-1755 (2000).
21. V. I. Kruglov, and J. D. Harvey, "Asymptotically exact parabolic solutions of the generalized nonlinear Schrödinger equation with varying parameters," J. Opt. Soc. Am. B **23**, 2541-2550 (2006).
22. C. Finot, and G. Millot, "Interactions of optical similaritons," Opt. Express **13**, 5825-5830 (2005).
23. A. C. Peacock, R. J. Kruhlak, J. D. Harvey, and J. M. Dudley, "Solitary pulse propagation in high gain optical fiber amplifiers with normal group velocity dispersion," Opt. Commun. **206**, 171-177 (2002).
24. P. H. Pioger, V. Couderc, P. Leproux, and P. A. Champert, "High spectral power density supercontinuum generation in a nonlinear fiber amplifier," Opt. Express **15**, 11358-11365 (2007).

1. Introduction

The generation of linearly-chirped parabolic pulses in optical fibers has motivated many studies in recent years [1]. To this end, an elegant approach consists in taking advantage of the asymptotic reshaping which occurs upon propagation in normally dispersive and nonlinear fiber amplifiers. Namely, any pulse tends to acquire the properties of an optical similariton [2]. Experimental demonstrations relying on amplification from either rare-earth doping [2] or Raman scattering [3] have confirmed the advantages of this method, especially when dealing with the generation of ultrashort, high peak power pulses.

Nevertheless, it is also of interest to study alternative methods of generating parabolic pulses, especially in the context of applications which do not target signal amplification, such as optical telecommunications [4-6]. Several specific techniques have been recently proposed: the use of superstructured fiber Bragg gratings which leads to passive pulse shaping [6]; the combination of two carefully chosen normally dispersive optical fibers [7]; and the use of an optical fiber whose *(absolute value of)* dispersion decreases along its length [8-10]. The latest approach is based on the observation that the longitudinal decrease of the normal dispersion is formally equivalent to optical gain [8]. In previous experiments, an effective dispersion decrease was approximated by a comb-like profile obtained from the concatenation of different segments of highly nonlinear fiber [10]: linearly chirped, parabolic intensity pulses sitting on exponentially decreasing wings were observed. Further experiments using a continuously tapered DDF were also recently reported [9], showing autocorrelation traces and pulse spectra which are consistent with the formation of parabolic pulses. However, the performances of such a configuration were limited by the impact of third-order dispersion and attenuation [11].

In this work we propose and experimentally demonstrate a hybrid nonlinear pulse shaping configuration that combines the advantages of using both Raman amplification and a dispersion-decreasing fiber *(DDF)*. To date, studies of hybrid configurations have been essentially confined to pulse shaping in the anomalous dispersion regime, in the context of adiabatic enhanced soliton pulse compression [12, 13] or, more recently, in the context of sech self-similar pulse evolution [14]. We demonstrate here that hybrid configurations can also be of great interest in the normal dispersion regime, with the purpose of generating self-similar parabolic pulses. By considering the nonlinear Schrödinger equation with a gain term and normal varying dispersion, we derive an optimal analytical design for the longitudinal decrease of the dispersion profile.

First, by considering passive propagation in a DDF, we show that parabolic pulses can be generated without amplification for a much more general class of dispersion profiles than previously known. As a matter of fact, we clarify the nature of the difference in pulse shaping between the forward and the backward *(i.e., with a continuous increase of dispersion)* propagation configurations. Our experiments enable us to obtain what is, to the best of our

#87110 - $15.00 USD Received 4 Sep 2007; revised 1 Oct 2007; accepted 3 Oct 2007; published 15 Nov 2007

knowledge, the first direct experimental demonstration of the generation of parabolic pulses via the use of a single dispersion-decreasing optical fiber taper.

Next we numerically and experimentally investigate in details the potential added benefits of using a hybrid configuration for parabolic pulse generation in the normal dispersion regime in a DDF with Raman gain. Namely, we demonstrate that adding gain in the DDF results in pulse propagation with a reduced temporal broadening, as well as with an increased spectral power density with respect to the passive case. A direct measurement of both the amplitude and phase of experimentally generated parabolic pulses in the active DDF clearly confirms the validity of our approach and theoretical predictions.

2. Fiber design

2.1 Analytical Design

We consider the longitudinal evolution of the complex electric field $\psi(z,T)$, which can be modelled by the nonlinear Schrödinger equation *(NLSE)* [15] :

$$i\,\frac{\partial \psi}{\partial z} \;=\; \frac{\beta_2}{2}\,\mathrm{D}(z)\;\frac{\partial^2 \psi}{\partial T^2} \;-\; \gamma\,|\psi|^2\;\psi \;+\; i\,\frac{g}{2}\,\psi\;, \tag{1}$$

where β_2 is the second order dispersion, γ is the nonlinear coefficient, and g is the linear distributed gain. T is the time in a co-propagating time frame, and z is the propagation distance.

In the normally dispersive case, Eq. (1) can be transformed into the following normalized form [7, 15] :

$$i\,\frac{\partial u}{\partial \xi} \;=\; \frac{1}{2}\,\mathrm{D}(z)\;\frac{\partial^2 u}{\partial \tau^2} \;-\; |u|^2\,u \;+\; i\,\frac{\Gamma_0}{2}\,u, \tag{2}$$

with u, τ, Γ_0 and ξ normalized parameters defined by :

$$u(\xi,\tau) \;=\; N\;\;U\;,\quad U(\xi,\tau) \;=\; \frac{\psi}{\sqrt{P_C}},\quad \tau \;=\; \frac{T}{T_0},\quad \xi \;=\; \frac{z}{L_D},\quad \Gamma_0 \;=\; g\;\;L_D, \tag{3}$$

where T_0 and P_C are the characteristic temporal width and peak power of the initial pulse, respectively. L_D, L_{NL} and N are the dispersion length, the nonlinear length and the "soliton" number, which are defined as :

$$L_D \;=\; \frac{T_0^2}{\beta_2},\qquad L_{NL} \;=\; \frac{1}{\gamma\;\;P_C},\qquad N \;=\; \sqrt{\frac{L_D}{L_{NL}}}. \tag{4}$$

We can then define the new distance ξ' and field u' coordinates as [8] :

$$u' \;=\; \frac{u}{\sqrt{\mathrm{D}(z)}}\qquad \text{and}\qquad \xi' \;=\; \int_0^{\xi}\;\mathrm{D}(X)\;\;dX\;, \tag{5}$$

#87110 - $15.00 USD Received 4 Sep 2007; revised 1 Oct 2007; accepted 3 Oct 2007; published 15 Nov 2007

so that we may transform (2) into the NLSE with constant *effective* gain Γ :

$$i\,\frac{\partial u'}{\partial \xi'} = \frac{1}{2}\,\frac{\partial^2 u'}{\partial \tau^2} - \left|u'\right|^2 u' + i\,\frac{\Gamma}{2}\,u' , \tag{6}$$

provided that $D(z)$ obeys the following Riccati equation :

$$\frac{d\,D}{d\xi} = \Gamma_0\ D - \Gamma\ D^2, \qquad D\,(\xi = 0) = 1 \tag{7}$$

The solution of the above equation (7) reads as :

$$D(\xi) = \frac{\Gamma_0}{\Gamma}\left\{ 1 + \frac{\Gamma - \Gamma_0}{\Gamma_0 + \Gamma\left(e^{\Gamma_0 \xi} - 1 \right)} \right\} \tag{8}$$

Let us note that in the limit case $\Gamma_0 \to 0$ *(passive configuration)*, the solution (8) becomes consistent with the hyperbolic decreasing profile proposed in [8] and used in [9, 10] :

$$D_0(\xi) = \frac{1}{1 + \Gamma\,\xi} \tag{9}$$

We can then see at this stage one of the major advantages of including a physical gain Γ_0. Parabolic pulse generation is an asymptotic characteristic of the NLSE propagation *(i.e., it is observed for* $\xi \to \infty$ [1] *)*, but in the passive configuration the efficiency of the reshaping is limited by linear losses and the impact of third-order dispersion, given that in this case the second-order dispersion asymptotically tends to zero *(Eq.* (9)*)* [11]. On the contrary, for a hybrid configuration those two bottlenecks can be removed: in this case D(z) will asymptotically tend to the non-zero value Γ_0 / Γ, thus limiting the potentially deleterious impact of higher-order dispersion terms, and preventing the formation of optical shocks.

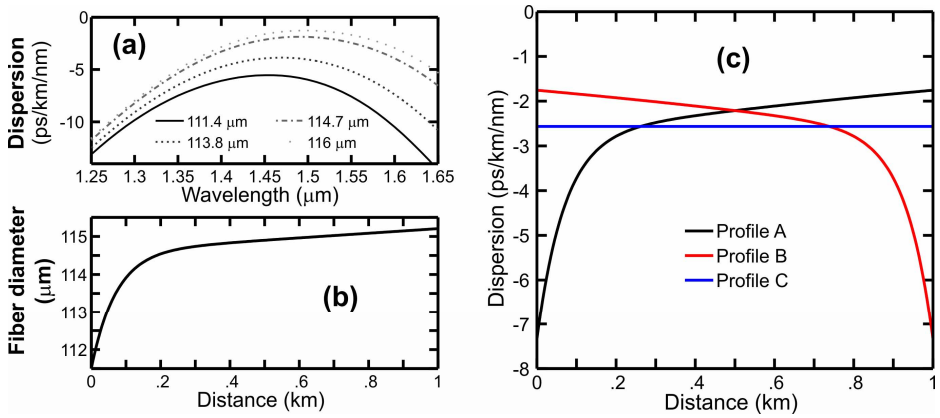

Fig 1. (a). Fiber dispersion versus wavelength for different outer fiber diameters. (b) Longitudinal evolution of the outer fiber diameter (c) Longitudinal evolution of the dispersion used in numerical simulations for different configurations: dispersion decreasing fiber (profile A, black line), dispersion increasing fiber (profile B, red line), uniform dispersion fiber (profile C, blue line).

2.2 Fiber drawing

Following the theoretical dispersion profile proposed by Eq. (8), we have drawn a 1-km long dispersion-decreasing optical fiber. The actual dispersion profile of the fiber was adapted to the Riccati profile of Eq. (8) with a physical gain G = 9.2 dB/km, an effective gain G_e = 46 dB/km, and to initial pulses with a full-width at half-maximum *(FWHM)* temporal width of 5 ps. As can be seen on Fig. 1(a), the dispersive properties of the fiber vary according

#87110 - $15.00 USD Received 4 Sep 2007; revised 1 Oct 2007; accepted 3 Oct 2007; published 15 Nov 2007

to the outer fiber diameter. Hence tailoring the longitudinal diameter [*Fig. 1(b)]* enables the control of the dispersion along the fiber. The drawing process was detailed in [16], and it involves a careful control of the fiber diameter by means of a digital feedback process. The resulting dispersion profile is plotted in Fig. 1(c) *(black solid line)*. As it can be seen, the dispersion values range from -7 ps/km/nm to -1.5 ps/km/nm *(values at 1560 nm)*, and the nonlinear coefficient γ is estimated to be 2.1 $W^{-1}.km^{-1}$. The linear loss of the DDF is 0.4 dB/km.

3. Experimental set-up

The experimental set-up that we have implemented in order to test our proposed parabolic pulse generation scheme is presented in Fig. 2. Initial sech pulses with a FWHM width of 5 ps were generated by a passively mode-locked fiber laser running at a repetition rate of 22 MHz at the central wavelength of 1558 nm. These pulses were amplified by an erbium doped fiber amplifier *(EDFA)*. An optical bandpass filter was used to remove amplified spontaneous emission induced by the EDFA. The peak power of the pulses could be adjusted by means of an optical variable attenuator. Next, the pulses were launched into the DDF: according to the direction of its connectorisation, we could test pulse propagation in the DDF in either configuration **A** or **B** *(the corresponding dispersion profiles are plotted in Fig. 1(c), black and red solid lines)*.

The gain in the DDF was provided through Raman amplification, which relies on the use of a continuous Raman fiber laser at 1455 nm as a pump source [17]. The linewidth of the pump laser was large enough to avoid Brillouin back-scattering effects. 2 W of average power could be delivered by the Raman fiber laser, out of which up to 1.4 W could be coupled into the DDF by means of a high-power WDM coupler. A backward pumping configuration was used in order to avoid local pump depletion effects [3, 18].

Our set-up was fully fibred and, with the exception of the specially designed DDF, all of our devices were commercially available and ready for use in telecommunications applications.

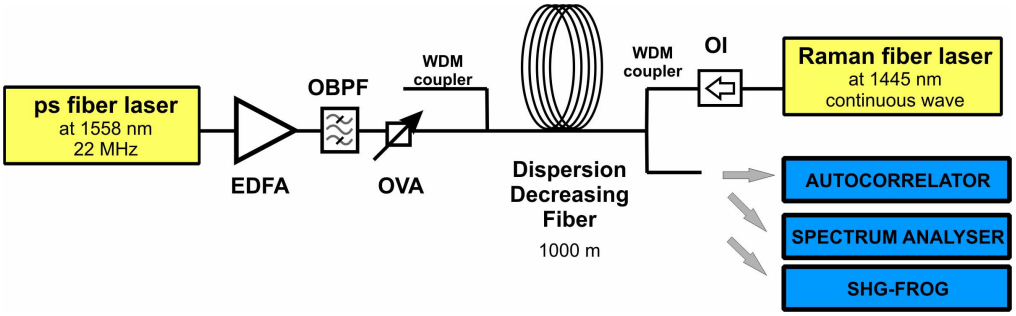

Fig 2. Experimental set-up. Erbium Doped Fiber Amplifier (EDFA), Optical BandPass Filter (OBPF), Optical Variable Attenuator (OVA), Optical Isolator (OI).

We characterized the pulses at the output of the DDF by recording their optical spectrum or their autocorrelation signal. We also used a FROG device *(Frequency Resolved Optical Gating based on second harmonic generation)* in order to characterize the output pulses both in amplitude and in phase [3, 19].

4. Results in a passive configuration

Let us first consider the evolution of the pulses in the DDF when used in a passive configuration *(i.e. without Raman pumping)*. We compare the results obtained for three different dispersion profiles [*plotted Fig. 1(c)]* : the profile **A**, where $|\beta_2(z)|$ progressively decreases; the profile **B,** where $|\beta_2(z)|$ increases with distance; and profile **C** which is a

#87110 - $15.00 USD Received 4 Sep 2007; revised 1 Oct 2007; accepted 3 Oct 2007; published 15 Nov 2007

constant dispersion profile, with a dispersion value corresponding to the average dispersion of both profiles **A** and **B**.

4.1 Numerical simulations

We numerically integrated Eq. (1) for an initial Gaussian pulse with 5 ps FWHM temporal width and 1 nJ energy. The resulting temporal intensity and chirp profiles as obtained after numerical propagation through 1000 m of fiber are plotted in Fig. 3(a). In configuration **A** *(solid black line)* we may see that a parabolic fit properly reproduces the entire pulse, including its wings. This means that in this case a parabolic pulse was generated, even though the dispersion profile of the fiber does not match the ideal theoretical profile which was proposed for such passive configuration *(Eq.* (9), [8]*)*. Let us note that the profile proposed by Eq. (8) is based on the assumption of obtaining a constant equivalent distributed gain Γ, with the help of a given level of physical gain Γ_0. However, it has also been demonstrated that parabolic pulse reshaping could also occur for nonuniform distributed gain [18, 20, 21]. Indeed, our simulations indicate that profile **A,** which can be associated to an equivalent gain decreasing profile in the passive case, could also be suitable for parabolic pulse generation.

Figure 3(a) shows that the dispersion profile (**A**, **B** or **C**) does not seem to have a crucial influence on the chirp profile. Quite to the contrary, the same figure demonstrates that the output pulse intensity profile is significantly influenced by the specific configuration which is used. Indeed, Fig. 3(a) reveals that profile **B** leads to a distorted and temporally much broader pulse than profile **A**. This observation may be qualitatively explained by taking into account the longitudinal evolution of the temporal [*Fig. 3(b)]* and spectral [*Fig. 3(c)]* width of the pulse. In case **B**, the dispersion acting on the pulse during the first stages of the propagation is low when compared with the other two configurations. Consequently, the pulse will undergo a relatively moderate temporal broadening [*Fig. 2(b)]*, which is associated to more efficient spectral broadening [*Fig 2(c)]*. Next, such a pulse with a broad spectrum will temporally broaden, which leads to a decrease of its peak-power and to the saturation of its spectral broadening. In the second part of the propagation, the pulse mainly undergoes a dispersive evolution. Since in this case the profile **B** exhibits the highest dispersion [*Fig. 1(c)]* combined with the largest spectral broadening, this configuration will naturally lead to the strongest temporal broadening in the final part of the propagation.

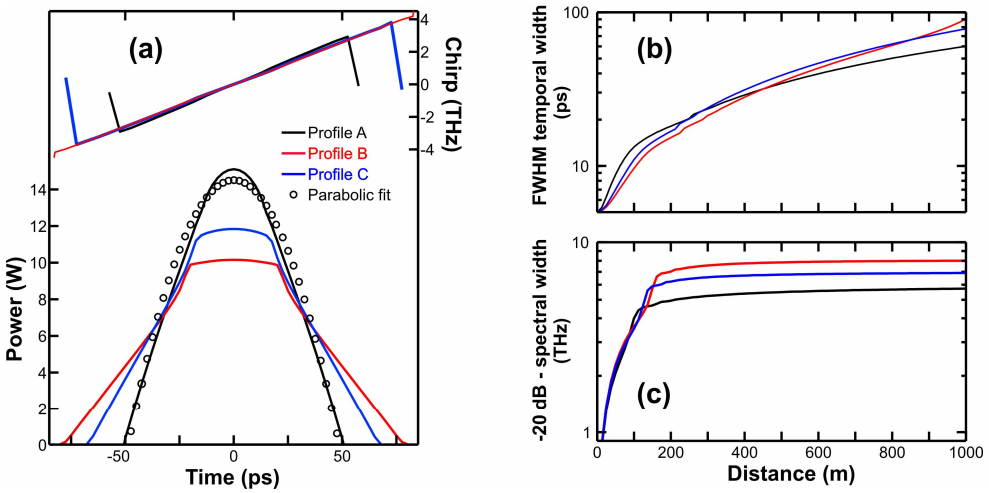

Fig. 3. Impact of the dispersion profile : Profile A (black line), profile B (red line) and profile C (blue line). (a) Temporal intensity and chirp profiles after propagation in 1000 m long fiber. Intensity profile obtained in profile A is compared to a parabolic fit (b) Longitudinal evolution of the FWHM temporal width; (c) Longitudinal evolution of the - 20 dB spectral width.

#87110 - $15.00 USD Received 4 Sep 2007; revised 1 Oct 2007; accepted 3 Oct 2007; published 15 Nov 2007

4.2 Experimental results

In the experimental test of the passive configuration, in order to avoid attenuation and extra self-phase modulation, we have removed the WDM couplers. The results of the FROG characterisation of the output pulses, for an initial pulse energy of 200 pJ, are plotted in Fig. 4 for the case of dispersion profile **A**. As it can be seen, the output pulse intensity profile is in good agreement with a parabolic fit, whereas its positive temporal chirp is strictly linear. The results of our FROG de-convolution were checked by usual methods such as their comparison with directly recorded autocorrelation and optical spectrum. Input pulses are shown to be in good agreement with a sech^2 fit *(Fig. 4, solid blue line)*.

For initial pulse energies higher than 200 pJ, the bandwidth limitations of our FROG device did not allow us to perform trustful measurements. Nevertheless, we could compare [*see Fig. 5(a) and 5(b)]* the experimentally recorded spectra with the results of numerical simulations, by taking as the initial condition a transform-limited sech pulse *(results for an initial energy of 1 nJ)*. The influence of the dispersion profile is clearly visible on the different shapes of the resulting spectra of Fig. 5(a). Similar results were also recently outlined in [9], but in those experiments the input pulse energy was limited to about 250 pJ, and the nature of the difference in pulse shaping between the forward and the backward propagation cases was not exhaustively clarified.

Figure 5(a) shows that for input energies of about 1 nJ the experimental spectra are nearly symmetric, which indicates that higher-order dispersion terms did not significantly affect pulse propagation in the DDF. Indeed, the observed slight spectral asymmetry in Figs. 5(a3) and 5(a4) could be well reproduced by additional simulations including the actual frequency-dependent dispersion profile of the DDF.

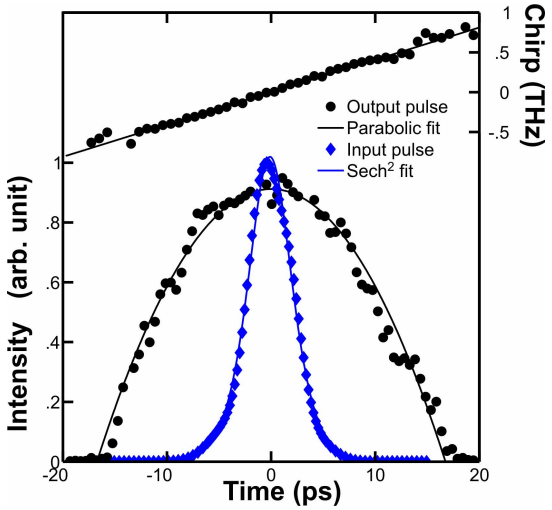

Fig. 4. Results of FROG characterisation of the input and output pulses (for an initial pulse energy of 200 pJ) : experimental intensity (bottom) and chirp (top) profiles compared to parabolic or sech fit.

We also studied the influence of the initial pulse energy on its output spectral and temporal broadening *[Fig. 5(b)]*. In agreement with the results of the previous subsection [*Fig. 3(b) and Fig. 3(c)]*, we can see in Fig. 5(b) that using profile **B** leads to pulses with larger temporal and spectral broadening than profile **A**. Experimental results were in good quantitative agreement with numerical predictions. The slight misfit of Fig. 4(b1) may be explained by the fact that in our experiments the pulses that we launched in the DDF were not quite transform-limited, owing to dispersive and nonlinear propagation effects occurring upon amplification in the EDFA.

#87110 - $15.00 USD Received 4 Sep 2007; revised 1 Oct 2007; accepted 3 Oct 2007; published 15 Nov 2007

The central part of the optical spectrum *(results plotted Fig. 6(a) for an initial pulse energy of 1.2 nJ)* exhibits, for both configurations, a remarkable flatness with fluctuations below 1 dB on a 2 THz span. Such a flatness removes the need of spectral equalization in applications such as spectral slicing [6] or pulse shaping [4]. Slightly higher power spectral density is achieved through the use of profile **A**.

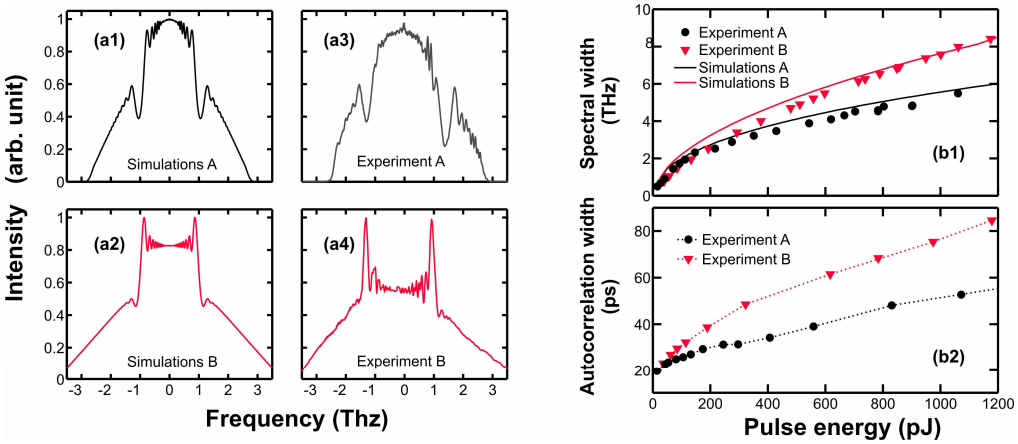

Fig. 5. (a). Comparison of the experimental spectra obtained in configuration A and B (1 nJ input pulse energy) with the results of numerical integration of NLSE; (b). Influence of the input pulse energy on the output pulse parameters : (b1) -20 dB spectral width (b2) temporal width (FWHM of autocorrelation signal).

Further experiments with input pulse energies of 2 nJ also showed that profile **B** is more sensitive to higher–order dispersive and nonlinear effects. Indeed, as it can be seen on Fig. 6(b), in the case of profile **A** the output spectrum is compact as it extends from -3 to 3.5 THz *(relative to the central frequency of the input fiber laser pulses)*. Quite to the contrary, we can observe in Fig. 6(b) that the other configuration leads to the first stages of a supercontinuum formation, with an output spectrum ranging from -12 THz to 5 THz. For slightly higher initial energies *(2.2 nJ, mixed red line)*, Figure 6(b) also shows that the spectral shape of the output pulse suffers a significantly larger degradation, indicating the full development of a broadband supercontinuum.

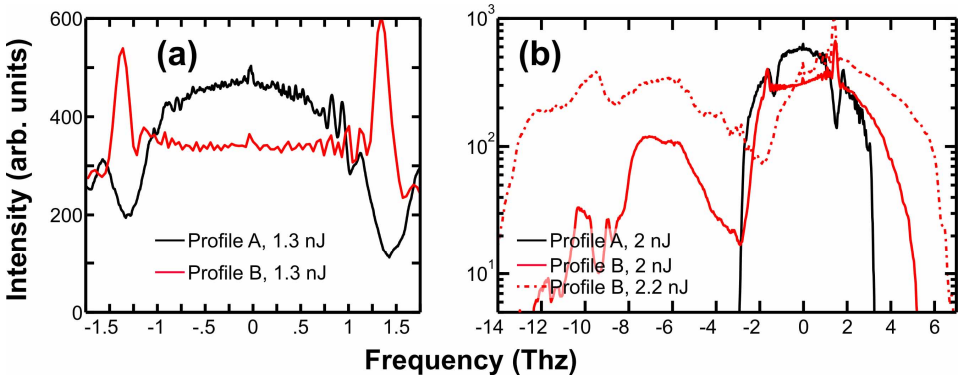

Fig. 6. Experimental optical spectra (0.7 nm resolution) obtained for profile A and B (black and red lines respectively). (a) central part of the spectra for an initial pulse energy of 1.2 nJ. (b) Spectra for input pulse energies of 2 and 2.2 nJ (solid and mixed lines respectively)

#87110 - $15.00 USD Received 4 Sep 2007; revised 1 Oct 2007; accepted 3 Oct 2007; published 15 Nov 2007

5. Results in presence of gain

Let us study now the evolution of the input pulses in presence of gain: we focus our attention here on the case of profile **A**.

5.1 Numerical simulations

We are interested to investigate at first the influence of the gain value on the reshaping of an initial 5-ps Gaussian pulse with the given initial energy of 200 pJ. Output temporal and spectral intensity profiles are plotted Fig. 7(a1) and 7(b1) for gain values ranging from 0 dB to 10 dB, respectively. We may notice in these figures that the higher the gain, the more parabolic is the output pulse, as already reported in [17]. Moreover, the spectral width of the pulse is also enhanced by the addition of distributed gain.

It is also of interest to compare the influence of gain on pulse reshaping, whenever the output pulse energy is kept constant. The corresponding results are plotted in Fig. 7(a2) and 7(b2), for an output pulse energy of 2 nJ. The results of Figs. 7(a2) and (b2) reveal some distinct features when compared with the case of constant input energy pulses of Figs. 7(a1) and 7(b1). Indeed it is clear that, for a given output pulse energy, using amplification leads to various advantages. First, it enables the use of lower initial pulse energies. Next, shorter parabolic pulses with an enhanced peak power are generated in the presence of gain. Moreover, the output spectrum is also narrower, which leads to higher power spectral densities.

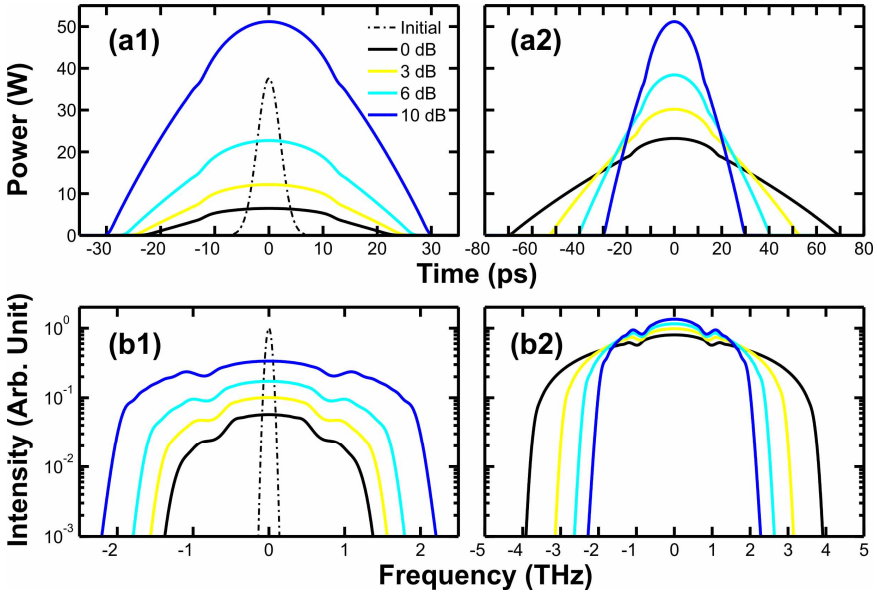

Fig. 7. Temporal and spectral intensity profiles at the output of the DDF [(a) and (b), respectively] in the presence of different integrated gain values : passive configuration, 3 dB, 6 dB and 10 dB gain (black, yellow, cyan and blue solid lines, respectively). The results are compared for either input pulses with the same energy [(a1) and (b1)] or for output pulses with the same energy [(a2) and (b2)].

In order to better understand the origin of the above observations, we numerically studied the longitudinal evolution of the pulse properties *(i.e., its spectral and temporal width, as well as peak-power)* for different gain values. Figure 8 compares simulation results obtained for pulses with the same output spectral width *(3.35 THz)*. These results were obtained for gains of 0, 3, 6, 10 and 15 dB, which correspond to initial pulse energies of 300, 240, 175, 100 and 37 pJ, respectively. From Fig. 8, we may point out that distributed gain has a significant

#87110 - $15.00 USD Received 4 Sep 2007; revised 1 Oct 2007; accepted 3 Oct 2007; published 15 Nov 2007

impact on the different properties of the longitudinal evolution of the pulses. Let us note at first in Fig. 8(a) that, for a passive configuration *(black solid curve)*, spectral broadening basically occurs in the first two hundred meters of the fiber and then saturates. To the contrary, in the presence of gain the initial peak power is reduced as the gain grows larger. As a result, Fig. 8(a) shows that the pulse spectral broadening is more evenly distributed along the DDF as the gain is increased: in the case of a 15-dB gain, we observe a nearly linear growth of the spectral width, with no saturation.

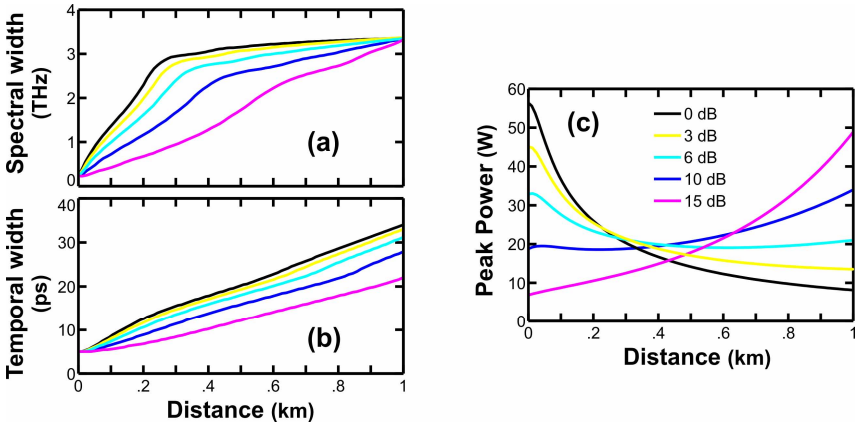

Fig. 8. Longitudinal evolution of the pulse properties for pulses with the same output spectral width. Evolution of the 20-dB spectral width (a), of the FWHM temporal width (b) and of the peak-power (c). Results are compared for different gain values : passive configuration, 3 dB, 6 dB, 10 dB and 15 dB gain (black, yellow, cyan, blue and pink solid lines respectively).

The analysis of the evolution of the pulse peak power which is plotted in Fig. 8(c) may also provide some interesting insight. For low gain values *(i.e., below 6-dB)*, the pulse peak power continuously decreases upon propagation down the fiber [*owing to the temporal broadening of the pulse as illustrated in Fig. 8(b)]*. For larger gain values, we can see from Fig. 8 that the lower initial spectral broadening leads a reduced temporal broadening as well. Moreover, the presence of gain may effectively counteract the action of temporal broadening, and eventually lead to a monotonic increase of the peak power. This "large gain" situation with a nearly linear increase with distance of both temporal and spectral widths is closer to the theoretically behaviour of self-similar pulses [1], as it could be expected given the physical gain value G = 9.2 dB which was chosen for the design the DDF profile *(see section 2, fiber design)*.

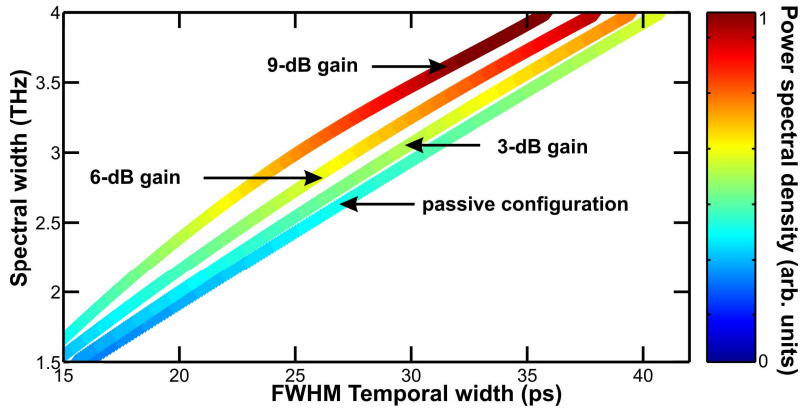

Fig. 9. Properties of the output parabolic pulses for different values of gain (0, 3, 6 and 9 dB) : -20-dB spectral width versus FWHM temporal width. The power spectral density is displayed by means of the colour map.

#87110 - $15.00 USD Received 4 Sep 2007; revised 1 Oct 2007; accepted 3 Oct 2007; published 15 Nov 2007

Finally, Fig. 9 provides a synthetic overview of some of the advantages of using a hybrid configuration for the generation of parabolic pulses. We have plotted here the output spectral width versus the output temporal width, for different gain values. From Fig. 9 it is clear that, for a given spectral broadening, the use of a hybrid configuration leads to shorter output pulses. This is of particular interest in the case of high-repetition rate signals, where the temporal broadening may lead to an interaction of neighbouring pulses, resulting with the generation of dark solitons in the overlap region [22]. Figure 9 also reveals that the average power spectral density in the 3-dB spectral bandwidth of the output pulse is enhanced by increasing the gain level, which can be useful if a further slicing of the parabolic continuum is targeted, for example whenever multi-channel parabolic pulse generation is envisaged [6].

5.2 Experimental results

We could carry out a FROG characterisation of the output pulses for the initial energy of 30 pJ. Raman gain was experimentally limited to 6-dB/km, which is less than the 9.2-dB/km optimal value that was considered in the fiber design. With similar arguments as the ones presented for the passive propagation case, we do not expect the mismatch between the optimal profile and the actual experimental conditions to heavily impair the generation of parabolic pulses by our set-up. Indeed, this mismatch will basically just lead to a nonuniform *(i.e, slowly decreasing)* longitudinal effective gain in Eq. (6). As a matter of fact, the retrieved intensity and chirp profiles of the generated parabolic pulses are plotted in Fig. 10. From these results we may verify that the output chirp is highly linear, and that the intensity profile is efficiently reshaped into a parabolic pulse. The output pulse has a FWHM temporal width of 20 ps, and an energy which is similar to that of the parabolic pulse which was generated in the passive configuration. As expected, the parabolic pulse generated in presence of gain is slightly shorter than the passively generated parabolic pulse *(FWHM temporal width of 23 ps)*. Let us note however that, when compared with the passive configuration, the inclusion of WDM couplers leads to a slightly larger nonlinear chirp of the initial pulse through self-phase modulation. This in turn introduces a slightly enhanced normal chirp of the initial pulses, which is ultimately beneficial for the parabolic reshaping.

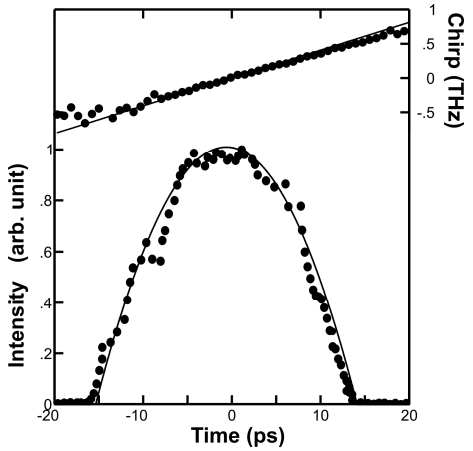

Fig. 10. Results of the FROG characterisation of the output pulse (for an initial pulse energy of 30 pJ) : experimental intensity profile (bottom) and chirp (top) profiles, compared to a parabolic and linear fit, respectively.

We also monitored the evolution of the output pulse properties as a function of the initial pulse energy. Our spectra and autocorrelation records enabled us to directly verify the numerical predictions whose overview was discussed in Fig. 9. The corresponding experimental results which are presented in Fig. 11 are in good qualitative agreement with the numerical simulations, which indeed confirms the benefits of our proposed hybrid

#87110 - $15.00 USD Received 4 Sep 2007; revised 1 Oct 2007; accepted 3 Oct 2007; published 15 Nov 2007

configuration with respect to the passive case. Namely, a reduced temporal broadening and a higher spectral density may be achieved by including distributed gain in a DDF.

The maximum output pulse energy and spectral width which can be achieved in a hybrid configuration are experimentally mainly limited by two factors. First, for large spectral broadenings, the effect of a finite gain-bandwidth becomes significant [23]. Next, we observed that for high initial pulse energies *(> 1 nJ)* Raman-assisted four wave-mixing between the signal and the continuous pump may occur.

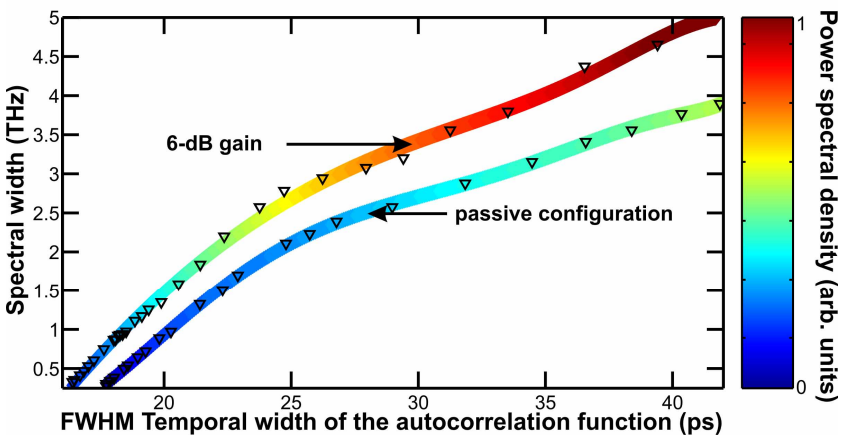

Fig. 11. Experimental properties of the output parabolic pulses for either passive or active (6-dB gain) DDF configurations : -20-dB spectral width versus the FWHM temporal width. The power spectral density is displayed by means of the colour map. Experimental data are plotted with triangles.

6. Conclusion

In conclusion, we experimentally demonstrated what is, to the best of our knowledge, the first direct experimental observation of the generation of parabolic pulses via the use of a single passive DDF. We performed a detailed comparison of the nonlinear pulse shaping that occurs in both forward and backward directions. We pointed out that profile **B** *(with dispersion increasing in absolute value)* leads to larger temporal distortions, as well as to greater temporal and spectral broadenings when compared with profile **A** *(with decreasing dispersion)*.

We have also shown the possibility of using a hybrid configuration, by combining the longitudinal dispersion evolution with physical gain. Efficient parabolic reshaping has been experimentally demonstrated in this case as well, and we outlined the potential benefits of such an approach. Indeed, deleterious third-order dispersion effects may be largely avoided by using a dispersion profile which asymptotically converges to a non-zero value. We have also shown that our hybrid approach may lead to higher spectral power densities, as well as to reduced temporal broadenings when compared with the passive configuration.

Although we carried out our experiments by exploiting Raman amplification, clearly similar results could be achieved by employing rare-earth doped fiber amplifiers with variable dispersion [12]. We may expect that the results of the present work may have further applications in the field of supercontinuum generation by means of active fibers [24].

Acknowledgments

We acknowledge fruitful discussions with P. Petropoulos, D. J. Richardson, Y. Jaouen and A. Maruta. This research was supported by the Agence Nationale de la Recherche *(SUPERCODE project)* and by the Conseil Régional de Bourgogne.

#87110 - $15.00 USD Received 4 Sep 2007; revised 1 Oct 2007; accepted 3 Oct 2007; published 15 Nov 2007